

Variable-node non-conforming membrane elements

Chang-Koon Choi†

Department of Civil and Environmental Engineering, Korea Advanced Institute of Science and Technology, Daejeon 305-701, Korea

Tae-Yeol Lee‡

Department of Civil and Environmental Engineering, University of California, Los Angeles, CA90095, USA

(Received January 24, 2003, Accepted July 15, 2003)

Abstract. Non-conforming membrane elements which have variable number of mid-side nodes with drilling degrees of freedom and which is designated as NMD_x have been presented in this paper. The non-conforming elements with variable number of mid-side nodes can be efficiently used in the local mesh refinement for the in-plane structures. To guarantee the developed elements always pass the patch test, the direct modification method is incorporated into the element formulation. Detailed numerical tests in this study show the validity of the variable node NC elements developed in this study and a wide applicability of these elements to practical problems.

Key words: direct modification method; drilling degrees of freedom; membrane element; transition element; variable node.

1. Introduction

The improved accuracy of a finite element can be obtained by the use of non-conforming (NC) modes which relax the interelement compatibility requirement. Following the pioneering works by Wilson *et al.* (1973) and Choi and Schnobrich (1975) several approaches have been proposed for the improvement of NC elements such as the modified Wilson NC element method (Taylor *et al.* 1976), natural formulation method (Argyris *et al.* 1980), free formulation method (Fellipa and Bergan 1987), and refined NC element method (RNEM) (Cheung and Chen 1995, Chen and Cheung 1997).

In many engineering practices, the stress concentration phenomena occur at the locations where the abrupt geometrical changes exist, or at the points of concentrated loading. For such problems, a finer mesh is required in the area of high stress gradients and a rather coarser mesh is used where the stress distribution is relatively uniform. To generate the local mesh refinement, the development and use of the variable-node transition NC elements, which effectively connect the refined and

† Institute Chair Professor

‡ Postdoctoral Researcher

unrefined meshes without generating hanging nodes, is attempted after the success in developing regular NC elements (Kim and Choi 1992, Choi *et al.* 2002c).

Choi and his co-workers have developed quadrilateral transition elements which have an additional node on the edge of a basic 4-node element (Choi and Park 1989, Choi and Lee 1995, Choi and Lee 1996). The behavior of this element was much improved by the addition of NC modes in the element formulations and was effectively used in the engineering problems, in particular in association with an adaptive mesh refinement. The use of NC modes generally improve the element behavior significantly, but at the same time it creates another problem that the resulting elements do not always pass the patch test because of the change in the strain energy due to the additional NC modes (Park and Choi 1997). To circumvent this defect, 'B-bar method' (Wilson and Ibrahimbegovic 1990) has been used in the element formulations by introducing correction matrix evaluated at every integration points, which requires additional computing efforts.

Recently, Choi *et al.* (2001) suggested the direct modification method (DMM) which corrects the NC elements to pass the patch test by introducing correction constants for the derivatives of NC modes. The fundamental concept of this method and applications to various element formulations can be found in the published literatures (Choi *et al.* 2001, Choi and Lee 2002a,b, Choi *et al.* 2002c, Choi and Lee 2003). Moreover, Lee and Choi (2002) utilized the DMM in developing a 5-node quadrilateral NC membrane element for modeling the transition zone between the refined and unrefined meshes. Their element behaved well but the mesh refinement by 5-node elements is limited to one-directional refinement pattern. In order to be more flexible and versatile for the element in generation of the transition zone, the extension of current 5-node element to include 6-node cases is desired.

The aims of this work are 1) to develop a 6-node quadrilateral membrane element that shows good performance and 2) to complete a series of variable node NC membrane elements which can be effectively used in the locally refined meshes with an easy modification from coarse meshes. Several numerical examples are analyzed to verify the performance of the proposed method.

2. Overview of non-conforming elements by direct modification method

2.1 Review of non-conforming elements

The total displacement field of an element which has additional NC displacement modes in addition to the ordinary conforming displacement modes can be expressed as

$$\mathbf{u} = \sum N_i \mathbf{u}_i + \sum \bar{N}_j \bar{\mathbf{u}}_j \quad (1)$$

in which N_i and \bar{N}_j are the conforming shape functions and the additional non-conforming modes, respectively, and \mathbf{u}_i and $\bar{\mathbf{u}}_j$ are the nodal displacements and additional unknowns corresponding to the NC modes, respectively. Some NC shape functions used in this study are shown in Fig. 1. The strain-displacement relation in the in-plane problem can be obtained in a usual manner, i.e., derivation of displacement fields in Eq. (1) and written as

$$\boldsymbol{\varepsilon} = \mathbf{B}\mathbf{u} + \bar{\mathbf{B}}\bar{\mathbf{u}} \quad (2)$$

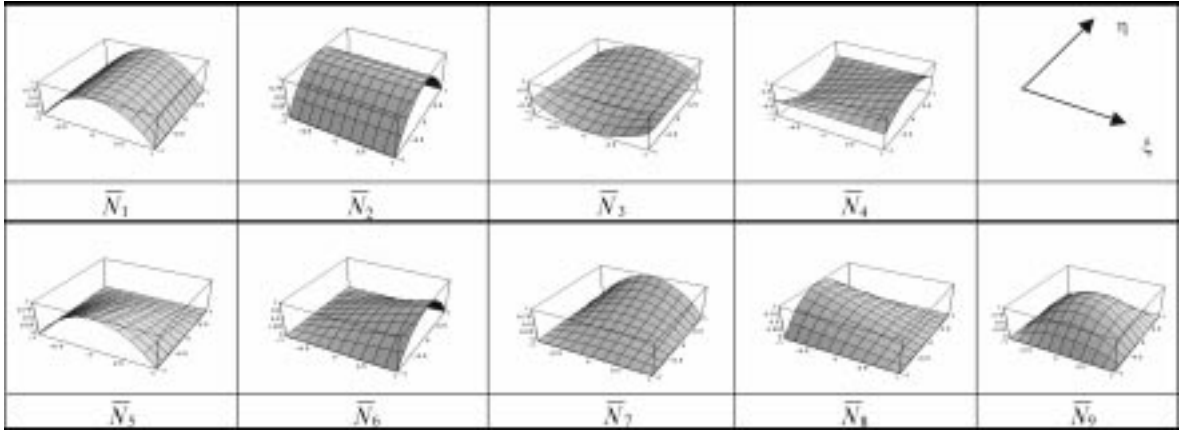


Fig. 1 Various NC modes

in which \mathbf{B} and $\bar{\mathbf{B}}$ are conforming and non-conforming part of strain-displacement matrix, respectively.

It is noted that the additional degrees of freedom $\bar{\mathbf{u}}$ in Eq. (2) are interpreted as the amplitudes of the added displacement modes rather than physical displacements at nodes and these internal degrees of freedom can be condensed out later. Since there are no loads corresponding to the internal degrees of freedom $\bar{\mathbf{u}}$, by rearranging the terms associated with \mathbf{u} and $\bar{\mathbf{u}}$ in the load-deflection equations, the equations may be partitioned as

$$\begin{bmatrix} \mathbf{K}_{cc} & \mathbf{K}_{cn} \\ \mathbf{K}_{cn}^T & \mathbf{K}_{nn} \end{bmatrix} \begin{Bmatrix} \mathbf{u} \\ \bar{\mathbf{u}} \end{Bmatrix} = \begin{Bmatrix} \mathbf{f} \\ \mathbf{0} \end{Bmatrix} \quad (3a)$$

where

$$\mathbf{K}_{cc} = \int_V \mathbf{B}^T \mathbf{D} \mathbf{B} dV, \quad \mathbf{K}_{cn} = \int_V \mathbf{B}^T \mathbf{D} \bar{\mathbf{B}} dV, \quad \text{and} \quad \mathbf{K}_{nn} = \int_V \bar{\mathbf{B}}^T \mathbf{D} \bar{\mathbf{B}} dV \quad (3b)$$

and the subscript c denotes conforming whereas n denotes non-conforming. The null sub-vector in the lower part of the load vector in Eq. (3a) indicates that no nodal loads can be applied in association with the NC modes. The enlarged element stiffness matrix in Eq. (3a) can be condensed back to the same size as the stiffness matrix of the ordinary conforming element \mathbf{K}_{cc} by using the static condensation procedures as

$$(\mathbf{K}_{cc} - \mathbf{K}_{cn} \mathbf{K}_{nn}^{-1} \mathbf{K}_{cn}^T) \mathbf{u} = \mathbf{f} \quad (4)$$

The elements formulated in the aforementioned manner, i.e., addition of NC modes, are designated as NC elements and show much improved behavior over original conforming element (Choi and Schnobrich 1975). This procedure can be applied to the in-plane elements. However, this type of elements was known not to always pass the patch test (Park and Choi 1997).

2.2 Application of direct modification method

To obtain the state of constant strain for an element to pass the patch test, the strain energy associated with NC modes should vanish in an element domain V in the fashion as shown in Eq. (5).

$$\int_V \bar{\mathbf{B}}^T dV = 0 \tag{5}$$

Recently, Choi *et al.* (2001) suggested the direct modification method (DMM) which set the NC modes free from patch test failure. The fundamental concept of this method and applications to 8-node hexahedral elements and 2-dimensional membrane elements with drilling degrees of freedom can be found in the published literatures (Choi *et al.* 2001, Choi *et al.* 2002c).

For the sake of better understanding, some important equations obtained by the DMM are repeated here as follows.

$$(\bar{N}_{j,x})^* = \left| \frac{\mathbf{J}(0,0)}{\mathbf{J}(\xi,\eta)} \right| \sum_{\alpha=1}^2 \left\{ J_{1\alpha}^{-1}(0,0) \left(\frac{\partial \bar{N}_j}{\partial \xi_\alpha} + c_{j\alpha} \right) \right\} \tag{6a}$$

$$(\bar{N}_{j,y})^* = \left| \frac{\mathbf{J}(0,0)}{\mathbf{J}(\xi,\eta)} \right| \sum_{\alpha=1}^2 \left\{ J_{2\alpha}^{-1}(0,0) \left(\frac{\partial \bar{N}_j}{\partial \xi_\alpha} + c_{j\alpha} \right) \right\} \tag{6b}$$

where the correction constants $c_{j\alpha}$ are defined in Eq. (7) and can be calculated analytically as

$$c_{j\alpha} = -\frac{1}{4} \int_{-1}^1 \int_{-1}^1 \frac{\partial \bar{N}_j}{\partial \xi_\alpha} d\xi d\eta \tag{7}$$

in which $\xi_1 = \xi$ and $\xi_2 = \eta$.

It is noted that the Eq. (7) can also be derived under the framework of the refined NC element method (RNEM) proposed by Cheung and his co-workers (Cheung and Chen 1995, Chen and Cheung 1997).

3. Variable-node non-conforming elements

3.1 Variable-node transition elements

Eqs. (8a) and (8b) are the shape functions for the elements with variable mid-side nodes as shown in Fig. 2.

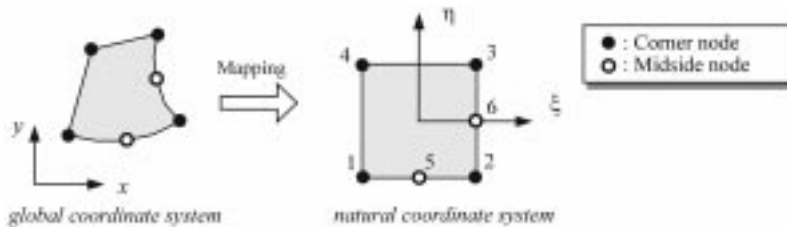


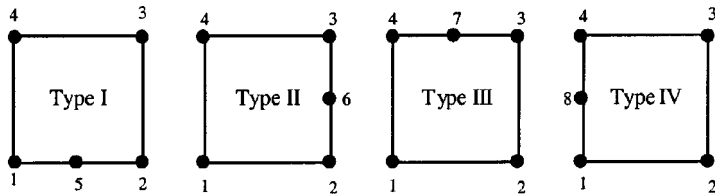
Fig. 2 Configuration of transition elements with variable midside nodes

$$\begin{aligned}
 N_1 &= N'_1 - \frac{1}{2}N_5 \\
 N_2 &= N'_2 - \frac{1}{2}(N_5 + N_6) \\
 N_3 &= N'_3 - \frac{1}{2}N_6 \\
 N_4 &= N'_4 \\
 N_5 &= \frac{1}{2}(1 - \xi^2)(1 - \eta) \\
 N_6 &= \frac{1}{2}(1 + \xi)(1 - \eta^2)
 \end{aligned} \tag{8a}$$

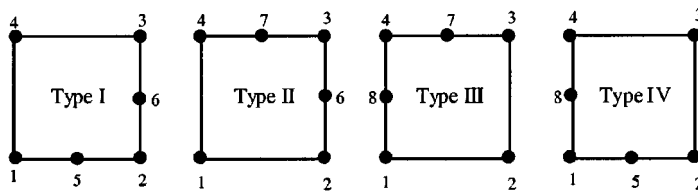
where

$$N'_i = \frac{1}{4}(1 + \xi_i\xi)(1 + \eta_i\eta), \text{ for } i = 1, 2, 3, 4 \tag{8b}$$

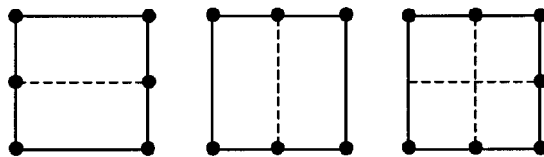
In Eqs. (8a) and (8b), the shape functions for mid-side nodes, i.e., N_5, N_6 , have non-zero values only when the corresponding mid-side nodes exist. Figs. 3(a) and 3(b) show the different types of



(a) 5-node elements



(b) 6-node elements



(c) division of an element

Fig. 3 Different type of transition elements

variable node elements generated based on the location of the mid-side node(s) relative to the basic corner nodes. The stiffness matrices of the Type-II to Type-IV element in Figs. 3(a) and 3(b) can be easily obtained by the proper transformation from that of the Type-I.

The 7-node element and some 6-node elements with particular mid-side node arrangements in Fig. 3(c) can be formulated in a similar manner but are not considered in this study as it is more convenient and efficient to subdivide them into two or four elements in practical use. Thus, only the formulations for Type-I elements in Fig. 3 are discussed in this paper.

3.2 Variable-node elements for in-plane problems

The interpolations for the displacements and rotations can be expressed by the same shape functions. However, the NC modes \bar{N}_j are added to displacements only as the excellent performance in the bending situation is expected (Choi *et al.* 2002c, Lee and Choi 2002). Thus, the interpolated displacement and rotation fields for the variable node membrane elements are expressed as

$$\mathbf{u} = \begin{Bmatrix} u \\ v \end{Bmatrix} = \sum_{i=1}^n N_i \mathbf{u}_i + \sum_{j=1}^m \bar{N}_j \bar{\mathbf{u}}_j \tag{9a}$$

$$\boldsymbol{\theta} = \theta = \sum_{i=1}^n N_i \theta_i \tag{9b}$$

where n is the number of nodes per element and m is the number of NC modes used.

The infinitesimal strains and rotations can be expressed by using differential operators as

$$\text{symm} \nabla \mathbf{u} = \sum_{i=1}^n \mathbf{B}_i \mathbf{u}_i + \sum_j \bar{\mathbf{B}}_j \bar{\mathbf{u}}_j = \mathbf{B} \mathbf{u}^e + \bar{\mathbf{B}} \bar{\mathbf{u}}^e \tag{10}$$

$$\boldsymbol{\theta} - \text{skew} \nabla \mathbf{u} = \sum_{i=1}^n N_i \boldsymbol{\theta}_i + \sum_{i=1}^n \mathbf{G}_i \mathbf{u}_i + \sum_j \bar{\mathbf{G}}_j \bar{\mathbf{u}}_j = \mathbf{G} \mathbf{u}^e + \mathbf{N} \boldsymbol{\theta}^e + \bar{\mathbf{G}} \bar{\mathbf{u}}^e \tag{11}$$

where \mathbf{B} and $\bar{\mathbf{B}}$ are the strain-displacement matrices of conforming part and NC part, respectively. $\mathbf{G}, \bar{\mathbf{G}}, \mathbf{N}$ are vectors defined as

$$\mathbf{G} = \langle -\frac{1}{2}N_{1,y} \quad \frac{1}{2}N_{1,x} \quad -\frac{1}{2}N_{2,y} \quad \frac{1}{2}N_{2,x} \quad \dots \quad -\frac{1}{2}N_{n,y} \quad \frac{1}{2}N_{n,x} \rangle \tag{12a}$$

$$\bar{\mathbf{G}} = \langle -\frac{1}{2}\bar{N}_{1,y} \quad \frac{1}{2}\bar{N}_{1,x} \quad -\frac{1}{2}\bar{N}_{2,y} \quad \frac{1}{2}\bar{N}_{2,x} \quad \dots \quad -\frac{1}{2}\bar{N}_{m,y} \quad \frac{1}{2}\bar{N}_{m,x} \rangle \tag{12b}$$

$$\mathbf{N} = \langle N_1 \quad N_2 \quad \dots \quad N_n \rangle \tag{12c}$$

When $\bar{\mathbf{B}}$ and $\bar{\mathbf{G}}$ are used without any modification, the element cannot always be guaranteed to pass the patch test due to the change of strain energy caused by addition of NC modes. To solve this problem, DMM (Choi *et al.* 2001) described briefly in Section 2.2 is adopted and the modified

matrices $\bar{\mathbf{B}}^*$ and $\bar{\mathbf{G}}^*$ in Eqs. (13b) and (13c) are obtained to replace $\bar{\mathbf{B}}$ and $\bar{\mathbf{G}}$ in Eqs. (10) and (11). Finally, the sub-matrices in Eq. (3) can be written as

$$\mathbf{K}_{cc} = \int_V \begin{bmatrix} \mathbf{B}^T \mathbf{D} \mathbf{B} & \mathbf{O} \\ \mathbf{O} & \mathbf{O} \end{bmatrix} dV + \alpha \mu \int_V \begin{bmatrix} \mathbf{G}^T \mathbf{G} & \mathbf{G}^T \mathbf{N} \\ \mathbf{N}^T \mathbf{G} & \mathbf{N}^T \mathbf{N} \end{bmatrix} dV \quad (13a)$$

$$\mathbf{K}_{cn} = \int_V \begin{bmatrix} \mathbf{B}^T \mathbf{D} \bar{\mathbf{B}}^* \\ \mathbf{O} \end{bmatrix} dV + \alpha \mu \int_V \begin{bmatrix} \mathbf{G}^T \bar{\mathbf{G}}^* \\ \mathbf{N}^T \bar{\mathbf{G}}^* \end{bmatrix} dV \quad (13b)$$

$$\mathbf{K}_{nn} = \int_V \bar{\mathbf{B}}^{*T} \mathbf{D} \bar{\mathbf{B}}^* dV + \alpha \mu \int_V \bar{\mathbf{G}}^{*T} \bar{\mathbf{G}}^* dV \quad (13c)$$

in which α is the problem dependent constant and $\alpha = 1$ is used in this study. As seen in the above equations, if α equals zero, the independent rotation field vanishes so that there are no rotational degrees of freedom considered.

Lee and Choi (2002) tested several integration schemes in developing NMD5-series elements to find the best performance element. In this paper, basically the same integration schemes are applied to NMD5-series elements (Lee and Choi 2002) are adopted to evaluate the stiffness matrices of NMD6-series elements.

Table 1 shows a series of NMD6-I to -VI elements, systematically established according to the NC modes added and the integration schemes used in the formulation. The development of the series of NMD-6 elements can be regarded as an addition to the family of NMD4 and NMD5 elements developed recently (Choi *et al.* 2002c, Lee and Choi 2002) and may complete the entire series of NMD elements. Here, the symbol NMD p - q is used to mean ' p -node Non-conforming Membrane element with Drilling degrees of freedom - Type q '.

Table 1 Types of membrane elements

| Elements | | Non-conforming modes | Integration schemes | | | | | | Remark |
|----------|----------|--|--------------------------------------|---|---|-----------------------------------|---|--|----------------------------|
| | | | \mathbf{K}_{cc} | | \mathbf{K}_{cn} | | \mathbf{K}_{nn} | | |
| | | u, v | $\mathbf{B}^T \mathbf{D} \mathbf{B}$ | $\begin{matrix} \mathbf{G}^T \mathbf{G} \\ \mathbf{G}^T \mathbf{N} \\ \mathbf{N}^T \mathbf{N} \end{matrix}$ | $\begin{matrix} \mathbf{B}^T \mathbf{D} \bar{\mathbf{B}}^* \\ \mathbf{G}^T \bar{\mathbf{G}}^* \end{matrix}$ | $\mathbf{N}^T \bar{\mathbf{G}}^*$ | $\bar{\mathbf{B}}^{*T} \mathbf{D} \bar{\mathbf{B}}^*$ | $\bar{\mathbf{G}}^{*T} \bar{\mathbf{G}}^*$ | |
| 4-node | NMD4 | $\bar{N}_1, \bar{N}_2, \bar{N}_3, \bar{N}_4$ | 2×2 | | 2×2 | 3×3 | 5-point | 2×2 | Choi <i>et al.</i> (2002c) |
| 5-node | NMD5 | $\bar{N}_2, \bar{N}_4, \bar{N}_7$ | 8-point | 3×3 | 8-point | 3×3 | 8-point | 3×3 | Lee and Choi (2002) |
| 6-node | NMD6-I | $\bar{N}_7, \bar{N}_8, \bar{N}_9$ | 3×3 | | 3×3 | | | 3×3 | This study |
| | NMD6-II | $\bar{N}_7, \bar{N}_8, \bar{N}_9$ | 3×3 | 2×2 | 2×2 | | | 2×2 | |
| | NMD6-III | $\bar{N}_7, \bar{N}_8, \bar{N}_9$ | 3×3 | 5-point | 2×2 | | | 2×2 | |
| | NMD6-IV | $\bar{N}_7, \bar{N}_8, \bar{N}_9$ | 3×3 | 5-point | 8-point | 3×3 | 8-point | 3×3 | |
| | NMD6-V | \bar{N}_7, \bar{N}_8 | 3×3 | 5-point | 8-point | 3×3 | 8-point | 3×3 | |
| | NMD6-VI | \bar{N}_7, \bar{N}_8 | 8-point | 3x3 | 8-point | 3×3 | 8-point | 3×3 | |

4. Numerical analysis

4.1 Eigenvalue test

In order to check the presence of spurious zero energy modes eigenvalue analyses of a single unconstrained stiffness matrix have been performed. Among the series of NMD6 elements the elements NMD6-I and NMD6-VI do not have spurious zero energy modes (Table 2) while the elements NMD6-II~NMD6-V have spurious zero energy modes. The elements with zero energy modes may show unstable solutions for some problems and must not be recommended for a practical use. However, for the purpose of comparison all the results of the presented elements are listed in the following sections.

4.2 Patch test

The patch test suggested by MacNeal and Harder (1985) has been modified to accommodate the mid-side nodes and carried out in order to check if the presented NMD6 series elements have the capability of representing constant strain states. Four patch test models composed of different combinations of 4-node, 5-node and 6-node elements are considered as shown in Fig. 4. The properties and dimensions used in this test are; Young's modulus $E = 1.0 \times 10^6$, Poisson's ratio $\mu = 0.25$, thickness $t = 0.001$, side length $a = 0.24$ and $b = 0.12$. Table 3 shows the locations of inner nodes in the patch and the mid-side nodes are located at the centers of element edges. The problems were solved with the prescribed displacement boundary and all the obtained results, including those of element which have spurious zero energy modes, are identical to the theoretical solutions (See Table 4).

Table 2 Eigenvalue test

| Elements | | Number of zero energy mode | Number of spurious zero energy mode | Remark |
|--------------|--------------|----------------------------|-------------------------------------|----------------------------|
| Node | ID | | | |
| 4-node | NMD4 | 3 | 0 | Choi <i>et al.</i> (2002c) |
| 5-node | NMD5 | 3 | 0 | Lee and Choi (2002) |
| | CLM(Type-I) | 3 | 0 | Choi and Lee (1995) |
| | CLM(Type-II) | 3 | 0 | |
| 6-node | NMD6-I | 3 | 0 | This study |
| | NMD6-II | 5 | 2 | |
| | NMD6-III | 4 | 1 | |
| | NMD6-IV | 5 | 2 | |
| | NMD6-V | 5 | 2 | |
| | NMD6-VI | 3 | 0 | |
| | CLM(Type-I) | 3 | 0 | |
| CLM(Type-II) | 3 | 0 | | |

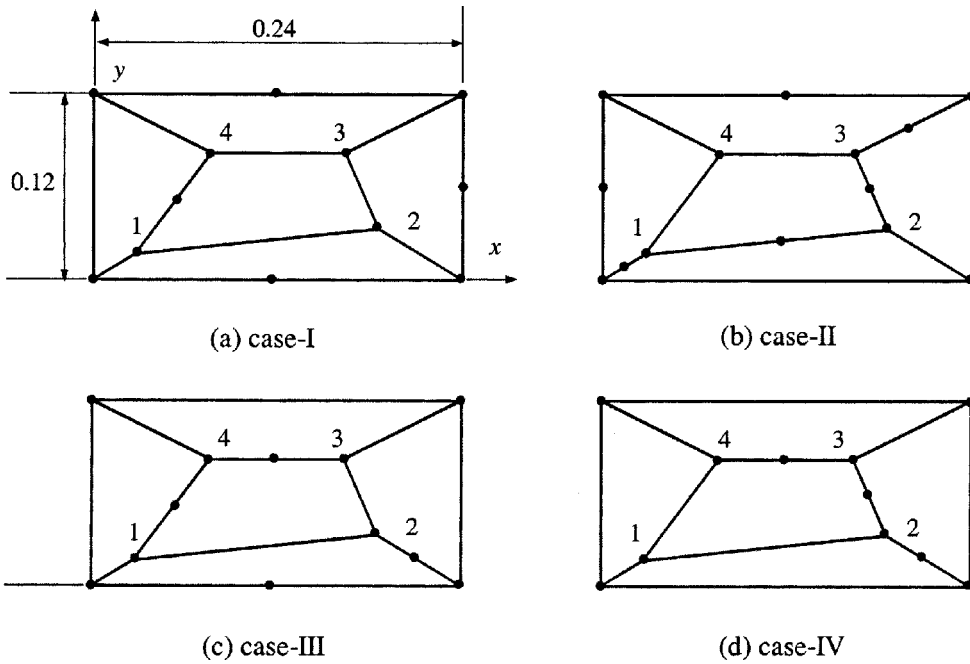


Fig. 4 Patch test

Table 3 Location of inner nodes

| Node | x | y |
|------|------|------|
| 1 | 0.04 | 0.02 |
| 2 | 0.18 | 0.03 |
| 3 | 0.16 | 0.08 |
| 4 | 0.08 | 0.08 |

Table 4 Boundary conditions and theoretical results

| Boundary conditions | Theoretical solutions |
|--|---|
| $u = 10^{-3}(x + y/2)$ $v = 10^{-3}(y + x/2)$ | $\epsilon_x = \epsilon_y = \gamma = 10^{-3}$ $\sigma_x = \sigma_y = 1333, \tau_{xy} = 400$ |

4.3 Cook's problem

This problem was originally proposed by Cook as a test for the accuracy of quadrilateral elements (Fig. 5) and has been frequently used to test new elements. Besides the shear dominant behavior, it also displays the effects of mesh distortion. The properties used in the test are; thickness $t = 1.0$, Young's modulus $E = 1.0$, and Poisson's ratio $\mu = 1/3$. The load $P = 1.0$ is distributed along the edge side. The results for the tip deflection at point A obtained by using various elements are compared

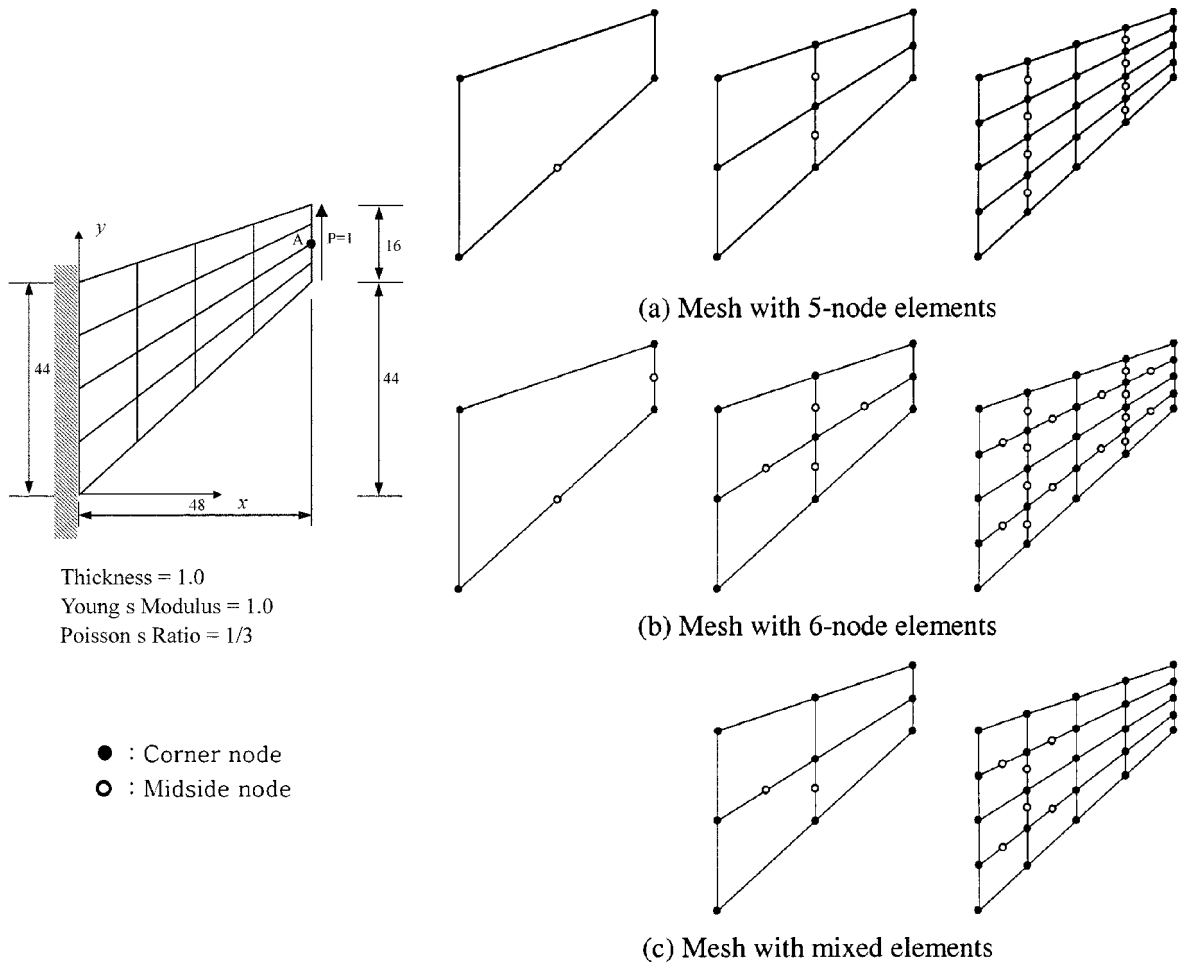


Fig. 5 Cook's membrane

with the reference value 23.91 obtained by numerical analysis for a refined model. Numerical tests with the sequentially refined meshes were also carried out to check the convergence of the new elements, and the test results are given in Table 5 along with those of other studies. All the types of elements, i.e., 4-node, 5-node, and 6-node elements, produced satisfactory results. It is interesting to note that the mixed model composed of 4-, 5-, 6-node elements can be used without generating any problems.

4.4 L-type panel

To show the validity and applicability of the presented elements, L-type panel under an uniform loads on the vertical side as shown in Fig. 6(a) is tested. The analyses were carried out using the mesh composed of elements with various number of nodes as shown in Fig. 6(b). In this test, NMD5 (Lee and Choi 2002) and NMD6-VI elements presented in this study are used together with NMD4 elements (Choi *et al.* 2002c). The material properties used are: Young's modulus $E = 10^5$

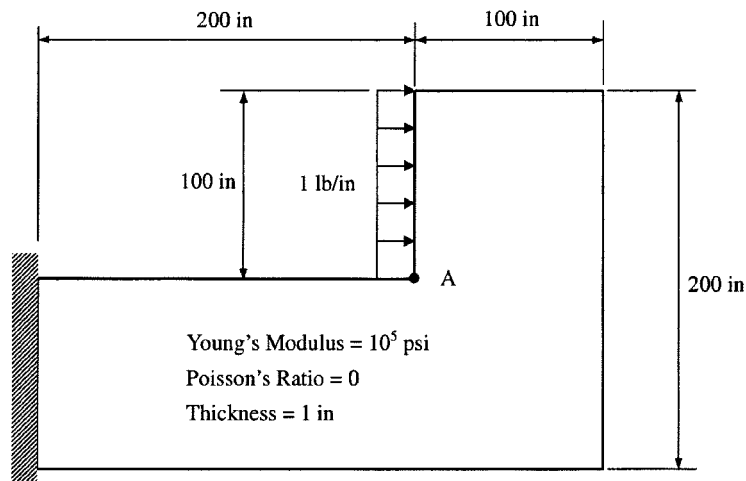
Table 5 Tip displacements of Cook's problem

| Elements | Mesh | | | Remark | |
|-----------------|--------------|-------|-------|--------|----------------------------|
| | 1 × 1 | 2 × 2 | 4 × 4 | | |
| 4-node | NMD4 | 16.72 | 22.97 | 23.67 | Choi <i>et al.</i> (2002c) |
| | NMS-4Mb | - | 20.33 | 22.88 | Choi <i>et al.</i> (1999) |
| | SQ4A | - | 17.31 | 21.66 | Choi and Paik (1994) |
| | M2 | - | 20.09 | 22.90 | Iura and Atluri (1992) |
| | MITC4 | - | 11.84 | 18.29 | Bathe and Dvorkin (1986) |
| 5-node | NMD5 | 20.47 | 21.07 | 23.18 | Lee and Choi (2002) |
| | CLM(Type-I) | 18.71 | 19.67 | 22.86 | Choi and Lee (1995) |
| | CLM(Type-II) | 19.63 | 19.88 | 22.95 | |
| 6-node | NMD6-I | 20.36 | 22.28 | 23.08 | This study |
| | NMD6-II | 20.78 | 21.42 | 23.29 | |
| | NMD6-III | 20.78 | 21.42 | 23.29 | |
| | NMD6-IV | 19.20 | 20.73 | 22.98 | |
| | NMD6-V | 18.58 | 20.10 | 22.53 | |
| | NMD6-VI | 20.51 | 22.88 | 23.22 | |
| | CLM(Type-I) | 18.88 | 20.83 | 23.13 | |
| CLM(Type-II) | 20.05 | 21.12 | 23.21 | | |
| Mixed | NMD4 | - | 21.23 | 22.95 | This study |
| | NMD5 | | | | |
| | NMD6-VI | | | | |
| Reference value | | 23.91 | | | |

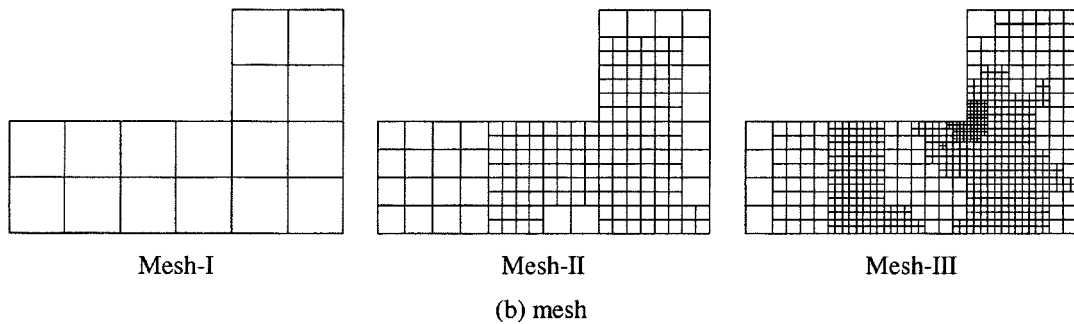
psi, and Poisson's ratio $\mu = 0$. The uniform load applied is $q = 1.0$ lb/in. Table 6 shows the stress σ_y at point A (Fig. 6(a)) obtained by different meshes and the reference value was obtained by the numerical analysis for a refined mesh using commercial software MSC/NASTRAN. Fig. 7(a) shows the deformed shapes of Mesh-I to -III with a scale of 500. The nodal stresses which are extrapolated from each Gauss points of the elements are averaged at each node and plotted in Fig. 7(b). To show the stress concentration near the point A more clearly, the contour is zoomed and illustrated together with the original contour. The number of elements (NEL) and total number of degrees of freedom (TDOF) used in the analyses are also listed in Table 6 for comparison. Even though a much smaller number of TDOF was used for Mesh-III the result from the Mesh-III (Fig. 7(b)) are almost the same as those from MSC/NASTRAN. The validity and effectiveness of the presented elements in local mesh refinement is well demonstrated by this numerical example.

5. Conclusions

A series of 6-node NC membrane elements with drilling degrees of freedom has been presented. Among the elements in the NMD6 series, the best performance was obtained by the element NMD6-VI as shown in the results obtained by tests conducted in this study (Tables 2,5, and 6).



(a) L-type panel



(b) mesh

Fig. 6 L-type panel

Table 6 Results of L-type panel

| | Stress σ_y at point A (psi) | NEL | TDOF | Remark |
|-----------------|------------------------------------|------|------|-------------|
| Mesh-I | 2.5 | 16 | 72 | |
| Mesh-II | 3.5 | 72 | 612 | This study |
| Mesh-III | 10.5 | 664 | 2265 | |
| Reference value | 10.6 | 4096 | 8448 | MSC/NASTRAN |

NEL : Number of **E**lementsTDOF : Total number of **D**egrees **O**f **F**reedom

Thus, the element NMD6-VI can be considered as the representative element of the entire elements in the NMD6-series and designated simply as NMD6 in the practical applications with the previously developed elements NMD4 and NMD5. The development of 6-node element presented in this study has made the family of NMD x (x -node Non-conforming Membrane element with **D**rilling degrees of freedom) complete and create a new category of elements termed "Variable Node Membrane Element". This type of elements are highly versatile in generating locally refined mesh and the generation of transition mesh which connect a finer zone and coarser zone. The validity and

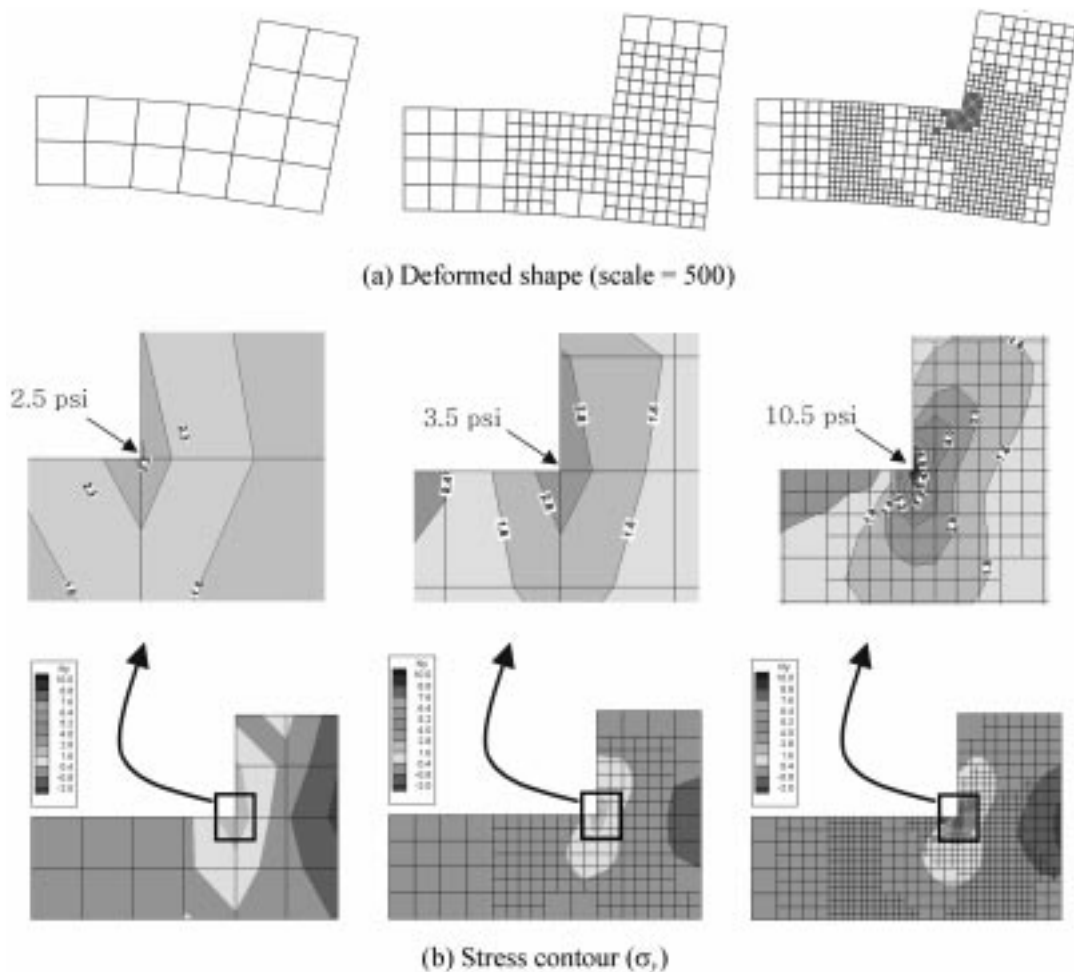


Fig. 7 Test results of L-type panel

applicability of these NMD x -series elements in local mesh refinement is well demonstrated by the practical examples such as ‘L-type panel’ for the in-plane problems.

Acknowledgements

The authors would like to thank the Korea Science and Engineering Foundation (KOSEF) for their partial support of this work through Smart Infra-Structure Technology Center (SISTeC) at Korea Advanced Institute of Science and Technology (KAIST).

References

Argyris, J.H., Hease, M. and Mlejnek, H.P. (1980), ‘On an unconventional but natural formulation of a stiffness

- matrix”, *Comp. Meth. Appl. Mech. Eng.*, **22**, 1-22.
- Bathe, K.J. and Dvorkin, E.N. (1986), “A formulation of general shell elements - the use of mixed interpolation of tensorial components”, *Int. J. Num. Meth. Eng.*, **22**, 697-722.
- Chen, W. and Cheung, Y.K. (1997), “Refined non-conforming quadrilateral thin plate bending element”, *Int. J. Num. Meth. Eng.*, **40**, 3919-3935.
- Cheung, Y.K. and Chen, W. (1995), “Refined nine-parameter triangular thin plate bending element by using refined direct stiffness methods”, *Int. J. Num. Meth. Eng.*, **38**, 283-298.
- Choi, C.K. and Park, Y.M. (1989), “Nonconforming transition plate bending elements with variable midside nodes”, *Comput. Struct.*, **32**, 295-304.
- Choi, C.K., Chung, K.Y. and Lee, T.Y. (2001), “A direct modification method for strains due to non-conforming modes”, *Struct. Eng. Mech.*, **11**(3), 325-340.
- Choi, C.K. and Lee, T.Y. (2002a), “Non-conforming modes for improvement of finite element performance”, *Struct. Eng. Mech.*, **14**(5), 595-610.
- Choi, C.K. and Lee, T.Y. (2002b), “Directly modified non-conforming modes for Mindlin plate-bending elements” *J. Eng. Mech.* ASCE, submitted.
- Choi, C.K., Lee, T.Y. and Chung, K.Y. (2002c), “Direct modification for non-conforming elements with drilling DOF”, *Int. J. Num. Meth. Eng.*, **55**, 1463-1476.
- Choi, C.K. and Lee, T.Y. (2003), “Efficient remedy for membrane locking of 4-node flat shell elements by non-conforming modes”, *Comp. Meth. Appl. Mech. Eng.*, **192**, 1961-1971.
- Choi, C.K. and Lee, W.H. (1995), “Transition membrane elements with drilling freedom for local mesh refinements”, *Struct. Eng. Mech.*, **3**(1), 75-89.
- Choi, C.K. and Lee, W.H. (1996), “Versatile variable-node flat shell element”, *J. Eng. Mech.* ASCE, **122**, 432-441.
- Choi, C.K. and Paik, J.G. (1994), “An efficient four node degenerated shell element based on the assumed covariant strain”, *Struct. Eng. Mech.*, **2**(1), 17-34.
- Choi, C.K. and Schnobrich, W.C. (1975), “Nonconforming finite element analysis of shells”, *J. Eng. Mech. Div.* ASCE, **101**, 447-464.
- Fellipa, C.A. and Bergan, P.G.. (1987), “A triangular bending element based on energy-orthogonal free formulation”, *Comp. Meth. Appl. Mech. Eng.*, **61**, 129-160.
- Iura, M. and Atluri, S.N. (1992), “Formulation of a membrane finite element with drilling degrees of freedom”, *Comput. Mech.*, **9**, 417-428.
- Kim, S.H. and Choi, C.K. (1992), “Improvement of quadratic finite-element for Mindlin plate bending”, *Int. J. Num. Meth. Eng.*, **34**(1), 197-208.
- Lee, T.Y. and Choi, C.K. (2002), “A new quadrilateral 5-node non-conforming membrane element with drilling DOF”, *Struct. Eng. Mech.*, **14**(6), 699-712.
- MacNeal, R.H. and Harder, R.L. (1985), “A proposed standard set of problems to test finite element accuracy”, *Finite Elem. Anal. Des.*, **1**, 3-20.
- Park, Y.M. and Choi, C.K. (1997), “The patch tests and convergence for nonconforming Mindlin plate bending elements”, *Struct. Eng. Mech.*, **5**(4), 471-490.
- Taylor, R.L., Beresford, P.L. and Wilson, E.L. (1976), “A non-conforming element for stress analysis”, *Int. J. Num. Meth. Eng.*, **10**, 1211-1219.
- Wilson, E.L. and Ibrahimbegovic, A. (1990), “Use of incompatible displacement modes for the calculation of element stiffnesses or stresses”, *Finite Elem. Anal. Des.*, **31**, 229-241.
- Wilson, E.L., Taylor, R.L., Doherty, W.P. and Ghaboussi, J. (1973), “Incompatible displacement models”, in *Numerical and Computer Models in Structural Mechanics*, eds. S.J. Fenves, N. Perrone, A.R. Robinson, and W.C. Schnobrich, Academic Press, New York, 43-57.